Disruption of the α5 Helix of Transducin Impairs Rhodopsin-Catalyzed Nucleotide Exchange†

Ethan P. Marin,‡ A. Gopala Krishna,‡,§ and Thomas P. Sakmar*,‡,§

Howard Hughes Medical Institute and Laboratory of Molecular Biology and Biochemistry, The Rockefeller University, New York, New York 10021

Received January 6, 2002; Revised Manuscript Received March 25, 2002

ABSTRACT: Photoactivated rhodopsin (R*) catalyzes nucleotide exchange by transducin, the heterotrimeric G protein of the rod cell. Recently, we showed that certain alanine replacement mutants of the α5 helix of the α subunit of transducin ($G\alpha_t$) displayed very rapid nucleotide exchange rates even in the absence of R* [Marin, E. P., Krishna, A. G., and Sakmar, T. P. (2001) *J. Biol. Chem. 276*, 27400−27405]. We suggested that R* catalyzes nucleotide exchange by perturbing residues on the α5 helix. Here, we characterize deletion, insertion, and proline replacement mutants of amino acid residues in α5. In general, the proline mutants exhibited rates of uncatalyzed nucleotide exchange that were 4−8-fold greater than wild type. The proline mutants also generally displayed decreased rates of R*-catalyzed activation. The degree of reduction of the activation rate correlated with the position of the residue replaced with proline. Mutants with replacement of residues at the amino terminus of α5 exhibited mild (<2-fold) decreases, whereas mutants with replacement of residues at the carboxyl terminus of α5 were completely resistant to R*-catalyzed activation. In addition, insertion of a single helical turn in the form of four alanine residues following Ile339 at the carboxyl terminus of α5 prevented R*-catalyzed activation. Together, the results provide evidence that α5 serves an important function in mediating R*-catalyzed nucleotide exchange. In particular, the data suggest the importance of the connection between the α5 helix and the adjacent carboxyl-terminal region of $G\alpha_t$.

The seven transmembrane G protein-coupled receptors (GPCRs)[1] form a large family of integral membrane proteins which detect extracellular signals and transmit them from outside to inside the cell (*1*). Classically, agonist-activated GPCRs transmit signals by catalyzing the activation of cytoplasmic heterotrimeric guanine nucleotide-binding regulatory proteins (G proteins). G proteins, which consist of α, *β*, and *γ* subunits, are activated by the exchange of bound GDP for GTP by the α subunit. The molecular mechanism underlying this crucial signal transduction event, the interaction between activated receptor and G protein, is not well understood.

Transducin (G_t), the heterotrimeric G protein of the vertebrate rod cell, exhibits nucleotide exchange rates that are extremely low (on the order of 10^{-3} min^{-1}) in the absence of photolyzed rhodopsin (R*) and very high in the presence of R*. These biochemical properties contribute to the low background noise and the high level of signal amplification that are the hallmarks of the highly sensitive rod cell (*2*). Crystal structures have been determined for the dark (or "off") state of rhodopsin (*3*), as well as for GDP- and GTP*γ*S-bound G_t (*4*−*6*). Although the structure of the complex between R* and G_t is not known, the sites on each molecule that interact have been identified by mutagenesis as well as peptide competition, antibody treatment, proteolysis, and other studies (*7*, *8*). The bulk of the data suggests that the cytoplasmic surface of R*, especially the second, third, and fourth cytoplasmic loops, interacts with a surface of G_t that includes the carboxyl termini of the α and *γ* subunits. These results suggest that R* is unlikely to contact directly the nucleotide-binding pocket of G_t and that R* must thus act "at a distance" to catalyze nucleotide exchange (*9*).

The α5 helix of the α subunit of G_t ($G\alpha_t$) has been implicated in mediating the mechanism of R*-catalyzed nucleotide exchange at a distance (*10*, *11*). The α5 helix connects the carboxyl-terminal region (CTR) of $G\alpha_t$, which is known to bind R* (*12*−*14*), to a loop that lies adjacent to the guanine ring of the nucleotide (Figure 1). The α5 helix has a hydrophobic buried surface that packs against the central *β* sheet and the α1 helix of $G\alpha_t$. The opposite surface is exposed to the solvent. The CTR, which comprises the last 11 amino acids (residues 340−350) of $G\alpha_t$, extends from

† This research was supported in part by the Allene Reuss Memorial Trust and National Institutes of Health Training Grants GM07739 and GM07982. T.P.S. is an Associate Investigator of the Howard Hughes Medical Institute.

* To whom correspondence should be addressed at Rockefeller University, 1230 York Ave., New York, NY 10021. Tel: 212-327-8288. Fax: 212-327-7904. E-mail: sakmar@mail.rockefeller.edu.

‡ Laboratory of Molecular Biology and Biochemistry, The Rockefeller University.

§ Howard Hughes Medical Institute, The Rockefeller University.

[1] Abbreviations: G protein, guanine nucleotide-binding regulatory protein; $G\alpha_t$, α subunit of transducin; $G\beta\gamma_t$, *βγ* subunits of transducin; CTR, carboxyl-terminal region (residues 340−350) of $G\alpha_t$; GPCR, G protein-coupled receptor; R*, active signaling conformation of rhodopsin.

10.1021/bi025514k CCC: $22.00
Published on Web 05/09/2002

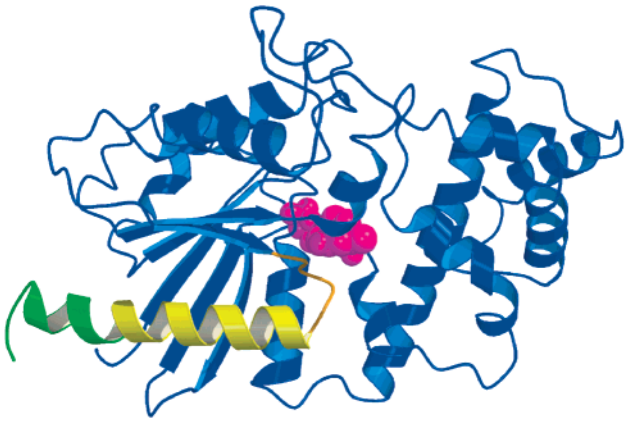

FIGURE 1: Overall view of the structure of $G\alpha_t$. The nucleotide (magenta) lies adjacent to the β6/α5 loop (orange) at the amino-terminal end of the α5 helix (residues 325−339, yellow). An NMR structure of a peptide corresponding to the carboxyl-terminal region (CTR) of $G\alpha_t$, residues 340−350, in the rhodopsin-bound conformation, is shown in green, docked onto the end of the α5 helix (*15*). (This region was not ordered in the crystal structure). This figure was prepared using the molecular graphics packages Molscript (*35*) and Raster3D (*36*) and the coordinates of the crystal structure of the GDP-bound heterotrimer of a $G\alpha_t/G\alpha_i$ chimera (*6*); the $G\beta\gamma_t$ subunits are not shown.

the α5 helix into the solvent. Although it is not well ordered in any of the available crystal structure of $G\alpha_t$, a NMR structure of the corresponding peptide bound to R* revealed an α-helical structure, which appeared to be a continuation of α5 that terminated in a reverse turn (*15*). We recently reported a detailed study of the rates of both basal (i.e., uncatalyzed) and R*-catalyzed nucleotide exchange in a series of alanine replacement mutants in α5 of $G\alpha_t$ (*16*). The results provided evidence that R* induces rapid release of GDP by perturbing several specific buried residues on α5, including Thr325, Val328, and Phe332.

In the present study, the role of the α5 helix in nucleotide exchange is further evaluated in a series of site-directed mutants designed to induce gross structural alterations in the helix. The mutant proteins were expressed in vitro and characterized by quantitative analysis of trypsin digest patterns. In general, these mutants, which included insertions of alanines into the helix as well as replacement of residues in the helix with prolines, exhibited increased rates of uncatalyzed nucleotide exchange and decreased rates of R*-catalyzed nucleotide exchange. Both results provide evidence for the involvement of α5 in mediating R*-catalyzed nucleotide exchange in G_t and specifically highlight the importance of functional coupling between the CTR and α5.

MATERIALS AND METHODS

Site-Directed Mutagenesis and in Vitro Expression of $G\alpha_t$. Site-directed mutations were created using the QuickChange system (Stratagene). The parent for all $G\alpha_t$ constructs was pGEM2sTα, the synthetic bovine $G\alpha_t$ gene cloned into the pGEM2 plasmid under control of a SP6 promoter (*17*). $G\alpha_t$ and $G\alpha_t$ mutant proteins were expressed in vitro in the presence of [^{35}S]methionine using the TNT Quick-Coupled transcription/ translation system (Promega). The translated products were passed over Bio-Spin 6 gel filtration spin columns (Bio-Rad) twice to remove excess nucleotides and [^{35}S]methionine. The volume of each sample was then adjusted to 100 μL in buffer A [5 mM Tris-HCl, pH 7.5, 150 mM NaCl, 2 mM $MgCl_2$, 1 mM DTT, 0.01% (w/v) *n*-dodecyl β-D-maltoside]. If the sample was to be studied in a R*-catalyzed assay, $G\beta\gamma_t$ [purified from bovine retinas as described (*18*)] was added to a final concentration of 30 nM. Every experiment was performed using freshly translated $G\alpha_t$.

Nucleotide Exchange Rate Assays. Samples (70 μL each) of translated $G\alpha_t$ or mutant $G\alpha_t$ kept on ice in buffer A were quickly warmed to room temperature in a water bath. For uncatalyzed exchange rate assays, the experiment was initiated by the addition of GTPγS to a final concentration of 100 μM. Five aliquots (8 μL) were withdrawn over the course of 6 h and digested. For R*-catalyzed assays, the experiment was initiated by the addition of a mixture of R* and GTPγS (4 μL) to a final concentration of 30 nM R* and 14 μM GTPγS. The rhodopsin was derived from urea-washed bovine rod outer segment membrane preparations that were solubilized in 1% (w/v) *n*-dodecyl β-D-maltoside as described (*19*). Immediately before addition to the reaction, the rhodopsin was photolyzed by illumination for 15 s with a fiber optic cable connected to a Dolan Jenner lamp equipped with a >495 nm long-pass filter. The samples were incubated at room temperature under illumination. Aliquots (8 μL) were withdrawn and digested at 1, 2, 3, 5, 10, and 20 min. For each sample studied, three control reactions were performed. One 8 μL aliquot was mock digested without trypsin. In addition, two 8 μL aliquots were digested following a 10 min incubation with GDP (100 μM) or a combination of GDP (100 μM), NaF (10 mM), and $AlCl_3$ (170 μM). The digestion procedure was adapted from Garcia et al. (*14*). Aliquots were mixed with 1.5 μL of digest buffer (5% Lubrol, 2 mM GDP, 1 mg/mL TPCK trypsin) and incubated on ice for 30 min. Digestion was terminated by the addition of 2.5 μL of termination solution (10 mg/mL aprotinin, 10 μM phenylmethanesulfonyl fluoride), followed by 6 μL of 3× SDS sample buffer (New England Biolabs). The proteolytic fragments were resolved by SDS−PAGE using precast 15% gels (Bio-Rad). The intensities of the fragments were quantitated by phosphorimaging using a storage phosphor screen, a Storm Imager, and ImageQuant software (Molecular Dynamics). $G\alpha_t$ in the GDP-bound inactive conformation yielded ~23 kDa fragments, and $G\alpha_t$ in the active conformation (GTPγS or GDP−AlF_4^- bound) yielded ~34 kDa fragments following trypsin digestion. The fraction of $G\alpha_t$ activated in a given sample was determined from the relative intensities of the two bands.

Data Analysis. Each data set from the uncatalyzed activation assay was fit to the exponential rise equation $y = c + 100[1 - \exp(-kt)]$. The half-time ($t_{1/2}$), the time at which 50% of the $G\alpha_t$ was activated, was calculated from the mean value of the rate constants derived from the exponential fits. The data for R*-catalyzed activation did not in all cases fit satisfactorily to a single exponential rise equation possibly due to the decay of R* that, in the case of slow-activating mutants, became apparent at later time points. Thus, the value for $t_{1/2}$ for R*-catalyzed activation was estimated for $G\alpha_t$ and each mutant by extrapolation from double exponential fits to the averaged data from three to five separate experiments.

A

```
                    330       340       350
Gαt          TDTQNVKFVFDAVTDIIIKENLKDCGLF
CT del 5     TDTQNVKFVFDAVTDIIIKENLK-----
CT del 10    TDTQNVKFVFDAVTDIII----------
CT del 25    TDT-------------------------
```

B

```
                    330           340           350
Gαt          TDTQNVKFVFDAVTDII----IKENLK----DCGLF
CT ala4      TDTQNVKFVFDAVTDII----IKENLKAAAADCGLF
α5 ala3      TDTQNVKFVFDAVTDIIAAA-IKENLK----DCGLF
α5 ala4      TDTQNVKFVFDAVTDIIAAAAIKENLK----DCGLF
α5 ile4      TDTQNVKFVFDAVTDIIIIIIIKENLK----DCGLF
```

FIGURE 2: Amino acid sequences of truncation and insertion mutants of $G\alpha_t$. The α5 helix includes residues 325−339, and the CTR includes residues 340−350. (A) Sequence alignment of truncation mutants of the carboxyl terminus of $G\alpha_t$. (B) Sequence alignment of insertion mutants of $G\alpha_t$.

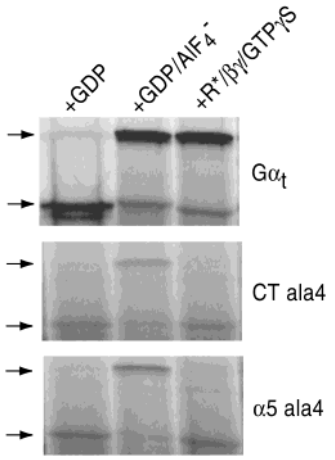

FIGURE 3: Trypsin proteolysis of wild-type $G\alpha_t$, CT ala4, and α5 ala4 following treatment for 10 min with either GDP (100 μM), a combination of GDP (100 mM), NaF (10 mM), and $AlCl_3$ (170 μM), or a combination of R* (30 nM), $G\beta\gamma_t$ (30 nM), and GTPγS (14 μM) (20 min incubation). The digested proteins, which were expressed in the presence of [^{35}S]methionine, were resolved by SDS−PAGE on 15% acrylamide gels and visualized by phosphorimaging. The arrows indicate the position of the ∼34 and ∼23 kDa bands. The CT ala4 and α5 ala4 insertion mutants were resistant to activation by R* and GTPγS. The results shown are representative of three separate experiments.

RESULTS

In an effort to test the role of the α5 helix in regulating nucleotide exchange in $G\alpha_t$, we introduced structural perturbations into the helix by site-directed mutagenesis. Three mutagenesis strategies were pursued: deletions, insertions, and proline scanning mutagenesis. Each of the mutants was expressed in vitro in a reticulocyte lysate-coupled transcription/translation system. The correct folding of the proteins, the ability to bind GDP, GTPγS, and GDP/AlF_4^-, and in some cases the rates of exchange of GDP for GTPγS were determined by quantitative analysis of trypsin digest patterns (*19*). Control experiments demonstrated the completeness and uniformity of trypsin digestions of all mutant proteins. When in vitro expressed $G\alpha_t$ is digested with trypsin, the size of the resulting fragment depends on the conformation of $G\alpha_t$ (*20*). When in the GDP-bound inactive state, the largest trypsin digest fragment is ∼23 kDa; following activation by either GDP/AlF_4^- or GTPγS, trypsin digestion instead yields an ∼34 kDa fragment. The relative intensities of these two bands were used to infer the conformation of the expressed mutant proteins and determine the rates of activation.

Deletions and Insertions in the α5 Helix and Carboxyl Terminus of $G\alpha_t$. Three deletion mutants were constructed in which 5, 10, or 25 amino acids were deleted from the carboxyl terminus of $G\alpha_t$ (Figure 2A). None of these constructs yielded proteins that could bind nucleotides as judged by trypsin digest analysis. Previously, it was reported that deletion of just the carboxyl-terminal amino acid (Phe350) from $G\alpha_t$ eliminated nucleotide binding (*13*). In contrast, a related G protein, $G\alpha_o$, was reported to tolerate a variety of deletions (*21*). It is not clear why $G\alpha_t$ is more sensitive than $G\alpha_o$ to deletions, but it might relate to the general difficulties in heterologously expressing functional $G\alpha_t$ (*22*).

Four insertion mutants were prepared (Figure 2B). In three of the mutants, the insertion point was immediately following Ile339. This position was chosen to minimize disruptions between the α5 helix and the rest of $G\alpha_t$. We attempted to insert a single helical turn using either three or four residues. Three alanines, four alanines, or four isoleucines were inserted at this location in three different constructs, called α5 ala3, α5 ala4, and α5 ile4, respectively. In the fourth mutant (called CT ala4), four alanine residues were inserted following residue 345 in the CTR. Alanines were used because of the reported propensity of this amino acid to form helices (*23*); isoleucines were inserted since residues 338−340 are isoleucine residues. Of these constructs, only the two with insertions of four alanines (CT ala4 and α5 ala4) consistently yielded proteins that could fold properly, and in these cases only a very small fraction of the total expressed protein could bind nucleotide. Trypsin digest analysis showed that CT ala4 and α5 ala4 could be activated by GDP/AlF_4^-; however, they appeared to be unresponsive to R*-catalyzed nucleotide exchange (Figure 3).

Proline Scanning Mutagenesis of the α5 Helix. Each residue in α5 (amino acids 325−339) was individually replaced by proline. Each of the resulting constructs yielded proteins of an appropriate molecular mass and expression level as judged by SDS−PAGE analysis of undigested samples (not shown). Several of the mutants were severely impaired in nucleotide binding, including N327P, V328P, K329P, V331P, F332P, and V335P. In these cases, the trypsin digestion patterns generally indicated that GDP binding was absent and that GTPγS binding was absent or significantly compromised. Additionally, AlF_4^--induced activation in these mutants was absent or greatly attenuated, presumably due to reduced GDP binding.

The proline mutants which could bind GDP were characterized in both uncatalyzed and R*-catalyzed activation assays. In the uncatalyzed assay (Figure 4), one mutant located in the first turn of the helix, T325P, exhibited an extremely fast activation rate that was 115 ± 13-fold greater than the activation rate of wild-type $G\alpha_t$ (Table 1). Several other proline substitution mutants exhibited moderately (from 4- to 8-fold) accelerated activation rates relative to that of $G\alpha_t$, including D333P, A334P, T336P, D337P, and I338P. The activation rates of three proline mutants, Q326P, F330P, and I339P, were similar to that of wild-type $G\alpha_t$. In the R*-catalyzed nucleotide exchange assay (Figure 5), the mutant T325P displayed rapid activation. All of the other proline

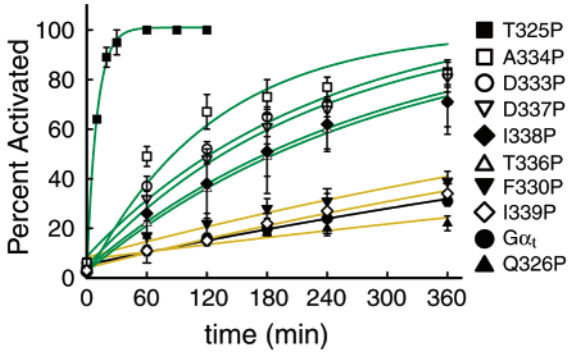

FIGURE 4: Uncatalyzed nucleotide exchange time courses of proline mutants in α5. $G\alpha_t$ and mutants were expressed in vitro and combined with 100 μM GTPγS. Aliquots (8 μL) were removed at the indicated times and digested with trypsin. The percent activation was determined by quantitative analysis of trypsin digestion patterns. The time zero data point is calculated from protein mixed with 100 μM GDP for 10 min. Each data point is the average of three to five independent experiments, and error bars depict ±2 × SEM. The solid lines represent fits to an exponential rise function. Wild-type $G\alpha_t$ is shown with a black line. Numerical values are presented in Table 1.

Table 1: Half-Times for Activation of $G\alpha_t$ and $G\alpha_t$ Mutants

mutant	uncatalyzed $t_{1/2}$[a] (min)	R*-catalyzed $t_{1/2}$[c] (min)
wild type	810 ± 66	1.1
T325P	7 ± 0.6	0.2
Q326P	1420 ± 242	1.8
N327P	ND[b]	ND
V328P	ND	ND
K329P	ND	ND
F330P	612 ± 47	1.5
V331P	ND	ND
F332P	ND	ND
D333P	160 ± 24	2.7
A334P	96 ± 41	3.1
V335P	ND	ND
T336P	211 ± 40	5.2
D337P	160 ± 32	12.4
I338P	189 ± 68	>30
I339P	668 ± 149	>30

[a] The half-time ($t_{1/2}$), the time at which 50% of the $G\alpha_t$ was activated, was calculated from the first-order rate constants derived from fits of each data set to the exponential rise equation $y = c + 100[1 - \exp(-kt)]$. Each mutant was assayed at least three times (WT $G\alpha_t$ was assayed 26 times), and an independent fit was made to each data set. The values reported are the mean $t_{1/2} \pm 2 \times$ SEM. [b] ND, not determined since the mutant protein did not fold properly. [c] The values for $t_{1/2}$ for R*-catalyzed activation were extrapolated from double exponential fits to the averaged data from three to five separate experiments.

mutants exhibited defects in activation that ranged from mild (e.g., Q326P) to very severe (e.g., I338P).

DISCUSSION

The mechanism by which R* catalyzes rapid nucleotide exchange by $G\alpha_t$ is not completely understood. Several different domains have been implicated in mediating activation. $G\beta\gamma_t$ subunits make direct contact with rhodopsin (*24*, *25*), and it has been proposed that the $G\beta\gamma_t$ subunits may transmit the activating signal from the receptor to the G protein (*9*, *26*). Recently, the feasibility of this βγ-based mechanism was demonstrated (*27*). Others have suggested that receptors alter interactions between the helical and ras-like domains of the G protein α subunit (*4*, *28*). However,

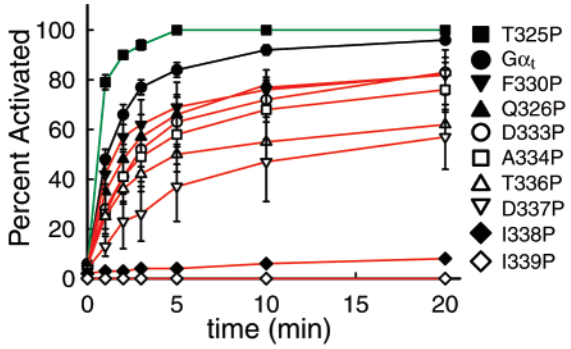

FIGURE 5: R*-catalyzed nucleotide exchange time courses of proline mutants in α5. $G\alpha_t$ and mutants were expressed in vitro and mixed with a combination of R* (30 nM), $G\beta\gamma_t$ (30 nM), and GTPγS (14 μM). The data were plotted as in Figure 4. The solid lines connect adjacent data points. Numerical values are presented in Table 1.

mutation of many of the residues in this region failed to uncover an important role for interdomain interactions in regulating nucleotide exchange in $G\alpha_t$ (*19*). The role of α5 in nucleotide exchange was suggested initially by its location as a link between the carboxyl-terminal tail of $G\alpha_t$, which binds to R*, and the nucleotide-contacting β6/α5 loop. Mutations in the carboxyl-terminal tail region disrupted R*−G_t binding (*13*) and R*-catalyzed activation (*14*), whereas a mutation in the β6/α5 loop simulated the action of R* by causing rapid nucleotide exchange (*29*, *30*). These results, in combination with sequence-based evolutionary analysis (*31*) and alanine scanning mutagenesis (*10*), led to the proposal that at least one mechanism of interaction between R* and the nucleotide involves alterations in the β6/α5 loop that are transmitted from the carboxyl terminus via the α5 helix.

We recently reported a study of the rates of both uncatalyzed and R*-catalyzed nucleotide exchange in mutants of $G\alpha_t$ in which residues in α5 were replaced with alanines (*16*). The data demonstrated that perturbation of residues Thr325, Val328, or Phe332 on the α5 helix itself would be sufficient to induce rapid nucleotide exchange and that R* likely induces conformational changes in α5. Perturbation of residues on α5 could propagate to nearby structures such as α1, β2, and β3 and from there to the nucleotide-binding pocket. To further characterize the function of α5 in mediating nucleotide exchange, we prepared and analyzed a set of $G\alpha_t$ mutants designed to introduce structural alterations into the α5 helix.

The replacement of residues in α5 with prolines was designed to cause structural changes in the helix. Prolines frequently introduce kinks into α helices, which bend away from the side of the helix containing the proline (*32*, *33*). The kinks arise in part because the side chain of proline bonds covalently to the backbone nitrogen and disrupts the typical pattern of hydrogen bonding in α helices between the backbone carbonyl oxygen of position $n - 4$ and the backbone N−H of position n. Prolines in positions 325−328 would not be expected to induce kinks per se since the $n - 4$ residue is absent. Accordingly, the Q326P mutant was similar to wild type in both the uncatalyzed and the R*-catalyzed activation assays (Figures 4 and 5).

The T325P mutant was an anomaly; it displayed very rapid nucleotide exchange in both uncatalyzed and R*-catalyzed nucleotide exchange assays. This mutation would not be

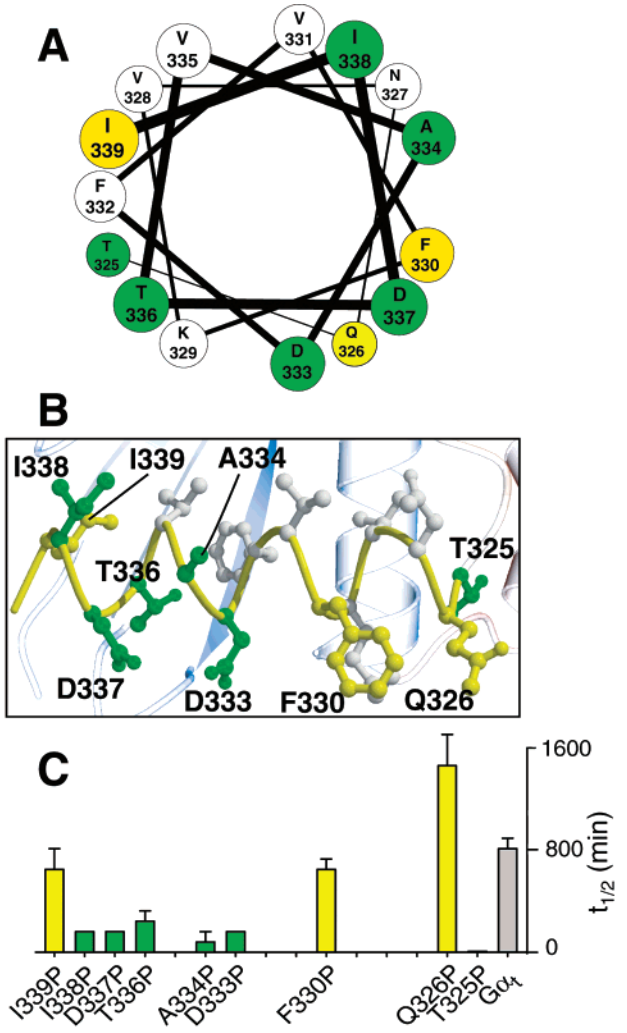

FIGURE 6: Schematic representation of the rates of uncatalyzed activation of proline mutants in α5. Residues are color coded by phenotype and match the colors of the lines in Figure 4: mutants similar to Gα$_t$ are in yellow, those exhibiting rates faster than Gα$_t$ are in green, and those slower than Gα$_t$ are in red. Residues that did not yield functional proteins when replaced with proline are colored white. (A) Helical wheel representation of α5, as viewed in from the carboxyl terminus looking toward the amino terminus; the surface stretching clockwise from Ile338 to Lys329 is solvent accessible. (B) Close-up of α5 in the GDP-bound crystal structure of Gα$_t$ (*5*), from the same angle as in Figure 1. (C) Histogram of the values for $t_{1/2}$ of activation for Gα$_t$ and proline replacement mutants.

expected to introduce a kink into α5 since it is the first residue in the helix. Instead, these results likely reflect the importance of the Thr325 side chain itself, which appears to stabilize the preceding β6/α5 loop by hydrogen bonding to Gln48. Consistently, the T325A mutant was found previously to display dramatically increased nucleotide exchange rates (*16*).

Several distinct patterns in the phenotypes of the proline substitution mutants are apparent. First, the six proline mutants that were not able to bind GDP were located predominantly on the buried surface of α5 (Figure 6A). Possibly, prolines in some of these positions caused bending of the helix away from the rest of Gα$_t$ so as to disrupt a large number of intramolecular contacts and to interfere with protein folding and/or stability. In the cases of N327P, V328P, and K329P, it is likely that the mutations disrupted important interactions involving the native side chains necessary to stabilize the first turn of α5 and thereby reduced the stability of the folded protein.

A second pattern is that the sites of the nine mutations which altered the rates of nucleotide exchange in both the uncatalyzed and the R*-catalyzed assays mapped to multiple surfaces of the α5 helix, including the solvent-exposed surface (Figures 6 and 7). This suggests that the effects of the proline substitution mutants on the nucleotide exchange rates were not merely due to disruption of contacts involving the substituted amino acid but that the prolines did in fact introduce structural alterations (e.g., kinks) into the helix. The data contrasted with the results of alanine scanning mutagenesis of the α5 helix (*16*). Alanine mutants would be expected to disrupt only interactions involving the side chain of the substituted residue. Accordingly, the sites of the alanine replacements that altered nucleotide exchange rates tended to cluster to particular surfaces of α5 that were involved in important interactions. In general, when a comparison of the phenotypes of the alanine and the proline replacement mutants of a given residue is possible, the proline mutant displayed faster uncatalyzed activation rates and slower R*-catalyzed activation rates than the corresponding alanine mutant. For example, replacement of residues Asp333 and Thr336 with alanine did not cause significant differences relative to wild type (*16*), whereas replacement of the same residues with proline led to measurable changes in both uncatalyzed and R*-catalyzed nucleotide exchange assays (Table 1).

A third pattern is that the effect on uncatalyzed activation rates was most pronounced for replacement of residues in the middle of the α5 helix (i.e., positions 333−338) with proline (Figure 6). Mutants at the carboxyl terminus (I339P) and the amino terminus (F330P) of the helix had milder phenotypes. These results are consistent with the introduction of kinks by the prolines. Kinks in the middle of the helix would be expected to be most disruptive of stabilizing interactions between α5 and the rest of Gα$_t$, whereas kinks at the ends would be expected to be least disruptive. These data also support the involvement of α5 in nucleotide exchange. The structure of Gα$_t$ has evolved for extremely low nucleotide exchange in the absence of R*. Therefore, one would predict that if α5 were indeed coupled to the nucleotide-binding pocket, perturbation of α5 would increase uncatalyzed activation rates.

A fourth pattern is that the proline mutants in α5 generally were found to exhibit reduced rates of R*-catalyzed activation. In particular, the defect in R*-catalyzed activation of the proline mutants increased as the proline was placed at positions progressively closer to the carboxyl-terminal end of the α5 helix (Figure 7). For example, the F330P mutant was only mildly defective, whereas the I338P mutant was nearly unresponsive to activation by R*. These results provide evidence that α5 is a key structure in the mechanism of R*-catalyzed nucleotide exchange and specifically that the link between the CTR and the α5 helix is critical. As additional evidence of the importance of this link, the α5 ala4 mutant (which would not be expected to have disrupted either α5 or the CTR directly) was resistant to activation by R* (Figure 3). It has also been reported recently that a G protein mutant with an insertion of five glycine residues following Ile339 was not activated by R* (*34*). Interestingly,

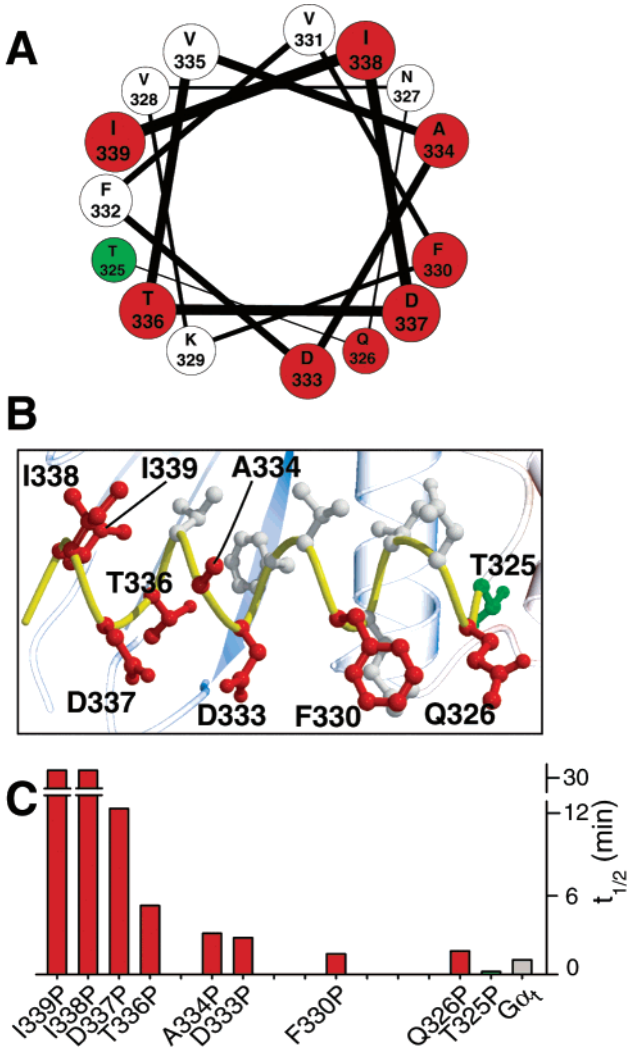

FIGURE 7: Schematic representation of the rates of R*-catalyzed activation of proline mutants in α5. The data are presented as in Figure 6. (A) Helical wheel diagram. (B) Close-up of the α5 structure. (C) Histogram of the values for $t_{1/2}$ of activation for $G\alpha_t$ and proline replacement mutants. The $t_{1/2}$ for I338P and I339P is >30-fold greater than that of wild-type $G\alpha_t$.

in the same report a mutant with an insertion of 11 amino acids corresponding to residues 329−339 of $G\alpha_t$ at the same spot could be activated by R*.

It is possible that the proline substitution mutations in α5 altered interactions between $G\alpha_t$ and $G\beta\gamma_t$ and thus indirectly affected R*-catalyzed activation. However, the fact that the site of the mutations is on the opposite face of the molecule from the known $G\beta\gamma_t$ binding surface argues against this possibility. Additionally, the observation that the defects in R*-catalyzed activation increased as the site of the proline substitution was moved toward the CTR also suggests that the dominant effect of the proline substitutions relates to disruption of R*-mediated effects.

The importance of the integrity of the CTR−α5 interface is consistent with two possible scenarios. First, the binding of R* to the CTR is transmitted to the nucleotide-binding pocket at least in part through residues on α5, so that disruption of the CTR−α5 junction interferes with this transmission. We previously presented evidence that R* does indeed communicate with the nucleotide via perturbation of several buried residues on α5 (*16*). Second, R* may bind directly to α5 as well as the CTR. Although it is well documented that R* binds to the carboxyl-terminal region of $G\alpha_t$ (*12*−*14*), it is not known how far this binding surface extends onto α5. Thus, the α5 ala4 mutants, as well as the I338P and I339P mutants, may have disrupted R*-catalyzed activation by preventing coordinated interactions between R* and both the CTR and α5 of $G\alpha_t$. Evidence for direct interaction between R* and α5 has been reported (*10*, *16*).

In summary, we tested the hypothesis that the α5 helix is a critical structure that controls nucleotide exchange in $G\alpha_t$. A variety of mutations was made to alter the structure of α5. We found that these mutants generally displayed increased rates of uncatalyzed nucleotide exchange and decreased rates of R*-catalyzed exchange. Both results suggest that α5 plays a critical role in the mechanism of nucleotide exchange by $G\alpha_t$.

ACKNOWLEDGMENT

We thank Eugene Simuni and Wing-Yee Fu for assistance with these studies and Dr. Boris Shraiman and members of the Sakmar Laboratory for helpful discussions.

REFERENCES

1. Gether, U. (2000) *Endocr. Rev. 21*, 90−113.
2. Menon, S. T., Han, M., and Sakmar, T. P. (2001) *Physiol. Rev. 81*, 1659−1688.
3. Palczewski, K., Kumasaka, T., Hori, T., Behnke, C. A., Motoshima, H., Fox, B. A., Le Trong, I., Teller, D. C., Okada, T., Stenkamp, R. E., Yamamoto, M., and Miyano, M. (2000) *Science 289*, 739−745.
4. Noel, J. P., Hamm, H. E., and Sigler, P. B. (1993) *Nature 366*, 654−663.
5. Lambright, D. G., Noel, J. P., Hamm, H. E., and Sigler, P. B. (1994) *Nature 369*, 621−628.
6. Lambright, D. G., Sondek, J., Bohm, A., Skiba, N. P., Hamm, H. E., and Sigler, P. B. (1996) *Nature 379*, 311−319.
7. Wess, J. (1997) *FASEB J. 11*, 346−354.
8. Helmreich, E. J., and Hofmann, K. P. (1996) *Biochim. Biophys. Acta 1286*, 285−322.
9. Iiri, T., Farfel, Z., and Bourne, H. R. (1998) *Nature 394*, 35−38.
10. Onrust, R., Herzmark, P., Chi, P., Garcia, P. D., Lichtarge, O., Kingsley, C., and Bourne, H. R. (1997) *Science 275*, 381−384.
11. Bourne, H. R. (1997) *Curr. Opin. Cell Biol. 9*, 134−142.
12. Hamm, H. E., Deretic, D., Arendt, A., Hargrave, P. A., Koenig, B., and Hofmann, K. P. (1988) *Science 241*, 832−835.
13. Osawa, S., and Weiss, E. R. (1995) *J. Biol. Chem. 270*, 31052−31058.
14. Garcia, P. D., Onrust, R., Bell, S. M., Sakmar, T. P., and Bourne, H. R. (1995) *EMBO J. 14*, 4460−4469.
15. Kisselev, O. G., Kao, J., Ponder, J. W., Fann, Y. C., Gautam, N., and Marshall, G. R. (1998) *Proc. Natl. Acad. Sci. U.S.A. 95*, 4270−4275.
16. Marin, E. P., Krishna, A. G., and Sakmar, T. P. (2001) *J. Biol. Chem. 276*, 27400−27405.
17. Sakmar, T. P., and Khorana, H. G. (1988) *Nucleic Acids Res. 16*, 6361−6372.
18. Marin, E. P., Krishna, A. G., Zvyaga, T. A., Isele, J., Siebert, F., and Sakmar, T. P. (2000) *J. Biol. Chem. 275*, 1930−1936.
19. Marin, E. P., Gopala Krishna, A., Archambault, V., Simuni, E., Fu, W.-Y., and Sakmar, T. P. (2001) *J. Biol. Chem. 276*, 23873−23880.
20. Fung, B. K., and Nash, C. R. (1983) *J. Biol. Chem. 258*, 10503−10510.
21. Denker, B. M., Schmidt, C. J., and Neer, E. J. (1992) *J. Biol. Chem. 267*, 9998−10002.
22. Min, K. C., Gravina, S. A., and Sakmar, T. P. (2000) *Protein Expression Purif. 20*, 514−526.

23. Chou, P. Y., and Fasman, G. D. (1978) *Annu. Rev. Biochem. 47*, 251−276.
24. Kisselev, O., and Gautam, N. (1993) *J. Biol. Chem. 268*, 24519−24522.
25. Kisselev, O. G., Ermolaeva, M. V., and Gautam, N. (1994) *J. Biol. Chem. 269*, 21399−21402.
26. Bohm, A., Gaudet, R., and Sigler, P. B. (1997) *Curr. Opin. Biotechnol. 8*, 480−487.
27. Rondard, P., Iiri, T., Srinivasan, S., Meng, E., Fujita, T., and Bourne, H. R. (2001) *Proc. Natl. Acad. Sci. U.S.A. 98*, 6150−6155.
28. Grishina, G., and Berlot, C. H. (1998) *J. Biol. Chem. 273*, 15053−15060.
29. Iiri, T., Herzmark, P., Nakamoto, J. M., van Dop, C., and Bourne, H. R. (1994) *Nature 371*, 164−168.
30. Posner, B. A., Mixon, M. B., Wall, M. A., Sprang, S. R., and Gilman, A. G. (1998) *J. Biol. Chem. 273*, 21752−21758.
31. Lichtarge, O., Bourne, H. R., and Cohen, F. E. (1996) *Proc. Natl. Acad. Sci. U.S.A. 93*, 7507−7511.
32. Barlow, D. J., and Thornton, J. M. (1988) *J. Mol. Biol. 201*, 601−619.
33. Woolfson, D. N., and Williams, D. H. (1990) *FEBS Lett. 277*, 185−188.
34. Natochin, M., Moussaif, M., and Artemyev, N. O. (2001) *J. Neurochem. 77*, 202−210.
35. Kraulis, P. J. (1991) *J. Appl. Crystallogr. 24*, 946−950.
36. Merritt, E. A., and Bacon, D. J. (1997) *Methods Enzymol. 277*, 505−524.

BI025514K